

The AP-2 Complex Is Excluded from the Dynamic Population of Plasma Membrane-associated Clathrin*[§]

Received for publication, August 27, 2003,
and in revised form, October 2, 2003
Published, JBC Papers in Press, October 6, 2003,
DOI 10.1074/jbc.C300390200

Joshua Z. Rappoport[‡], Bushra W. Taha[‡],
Simone Lemeers[§], Alexandre Benmerah[§],
and Sanford M. Simon[‡]¶

From [‡]The Laboratory of Cellular Biophysics, The Rockefeller University, New York, New York 10021 and the [§]Department of Infectious Diseases, Institut Cochin (INSERM U567, CNRS UMR 8104, Université Paris 5), 27 rue du Faubourg St. Jacques, 75014 Paris, France

Numerous biologically relevant substrates are selectively internalized via clathrin-mediated endocytosis. At the plasma membrane the AP-2 complex plays a major role in clathrin coat formation, interacting with both cargo and clathrin. Utilizing simultaneous dual-channel total internal reflection fluorescence microscopy we have analyzed components of the AP-2 complex (α - and β 2-adaptin) during clathrin-mediated endocytosis. Although in static images enhanced green fluorescent protein-tagged AP-2 markers significantly co-localized with clathrin and other components of clathrin-coated pits, AP-2 did not seem to be present in clathrin spots that appeared to undergo internalization or motility parallel to the plane of the plasma membrane. Two populations of clathrin at the plasma membrane seem to exist, the dynamic and the static, and AP-2 appears to be only found within the latter. These results suggest that co-localized clathrin/AP-2 puncta may represent loci for coated pit production and that previous models that assumed AP-2 was retained within clathrin coats during endocytosis may need to be re-evaluated.

Clathrin-mediated endocytosis is involved in internalization of receptors and ligands, cell adhesion molecules, and the synaptic vesicle cycle (1–7). Clathrin-coated vesicle formation requires recruitment of adaptor protein complexes (APs)¹ and

* This work was supported by “Association de Recherche contre le Cancer” Grant 4727 (to A. B.), National Science Foundation Grants BES-0110070 and BES-0119468 (to S. M. S.), and National Institutes of Health Grant 1 F32 GM069200-01 (to J. Z. R.). The costs of publication of this article were defrayed in part by the payment of page charges. This article must therefore be hereby marked “advertisement” in accordance with 18 U.S.C. Section 1734 solely to indicate this fact.

[§] The on-line version of this article (available at <http://www.jbc.org>) contains Supplemental Material (Video 1 and two supplemental figures).

¶ To whom correspondence should be addressed: The Laboratory of Cellular Biophysics, The Rockefeller University, 1230 York Ave., Box 304, New York, NY 10021. Tel.: 212-327-8130; Fax: 212-327-7543; E-mail: simon@rockefeller.edu.

¹ The abbreviations used are: AP, adaptor protein; TIR-FM, total internal reflection fluorescence microscopy; DMEM, Dulbecco’s modified Eagle’s medium; Tf, transferrin; Tfr, transferrin receptor; LDL, low density lipoprotein; DiI, 1,1’-dioctadecyl-3,3,3’,3’-tetramethylindocarbocyanine.

accessory proteins onto the donor membrane, assembly of clathrin coats, induction of membrane curvature, and fission of the mature bud (8–11). AP-2 is involved in the formation of clathrin coats at the plasma membrane and links receptor internalization to clathrin assembly. This complex consists of large subunits, α - and β 2-adaptins, and two smaller ones, μ 2 and σ 2, and has some structural similarity to AP-1 and AP-3 involved in clathrin coat production at the trans-Golgi and endosomes, respectively (12).

Since the original description of clathrin (13), a great deal of information has been gained from co-localization experiments, bulk measurements of endocytosis and *in vitro* reconstitution (14–16). These techniques are limited in real-time kinetic information regarding the production of individual clathrin-coated vesicles. Recently, time-lapse epifluorescence microscopy studies have provided important insights into this process. For example, clathrin-coated vesicles appear to form only in restricted areas of the plasma membrane (17) and agonist-activated G-protein coupled receptors target to pre-existing clathrin-coated pits for internalization, as opposed to inducing coat formation *de novo* (18, 19). The technique of total internal reflection fluorescence microscopy (TIR-FM) provides a sensitive approach to examine events near the plasma membrane such as exocytosis, cell adhesion, and cytoskeletal organization (20–22). More recently, work by our laboratory and others has demonstrated that TIR-FM is a suitable system for analysis of molecules involved in clathrin-mediated endocytosis (23–25).

The present studies have extended our analysis of endocytosis to the AP-2 complex. Using dual-color TIR-FM to analyze the dynamics of clathrin and AP-2 in live cells, we have observed strong spatial co-localization between dsRed-clathrin and markers for AP-2. However, this correlation only holds for the static population of clathrin spots. AP-2 was not found in dynamic puncta, laterally mobile or internalized. Thus, these two populations of clathrin may be functionally distinct, and although AP-2 may be involved in the production of clathrin coats, it does not seem to be retained during the process of endocytosis.

EXPERIMENTAL PROCEDURES

Plasmid Constructs and Cell Culture—EGFP- α C-adaptin was generated by transferring the full-length mouse α C cDNA from the pACT2 vector (a gift of Dr. Juan Bonifacino, National Institutes of Health, Bethesda, MD) downstream and in frame with EGFP in pEGFP-C2 vector (Clontech) using the BglII and SalI. dsRed-clathrin (rat light chain α) was a gift of Dr. Thomas Kirchhausen, Harvard Medical School, Boston, MA. EGFP- β 2-adaptin was a gift of Dr. Marc G. Caron, Duke University, Durham, NC). HeLa cells were maintained in DMEM (Mediatech Cellgro, Herndon, VA) with 10% fetal bovine serum in a 37 °C incubator humidified with 5% CO₂ and were imaged 48 h post-transfection with either Fugene6 (Roche Diagnostics) or the Calcium Phosphate kit (Invitrogen).

Immunocytochemistry—Immunocytochemistry was performed as described previously (26, 27). Primary antibodies included anti-transferrin receptor (Tfr) (CD71) and anti- γ -adaptin 100.3 and anti- β -adaptins 100.1 mouse monoclonal antibodies (Sigma), anti-CALM (C-18) and anti-Epsin (R-20) goat polyclonal antibodies (Santa Cruz Biotechnology, Santa Cruz, CA), anti-clathrin (derived from the CON.1 hybridoma (ATCC, Manassas, VA)) and anti-Eps15 (3T, a gift of Dr. Pier Di Fiore, European Institute of Oncology, Milan, Italy). Alexa-Fluor594-labeled goat anti-mouse and donkey anti-goat immunoglobulins were from Molecular Probes (Eugene, OR). Samples were examined under an epifluorescence microscope (Leica) with a cooled CCD camera

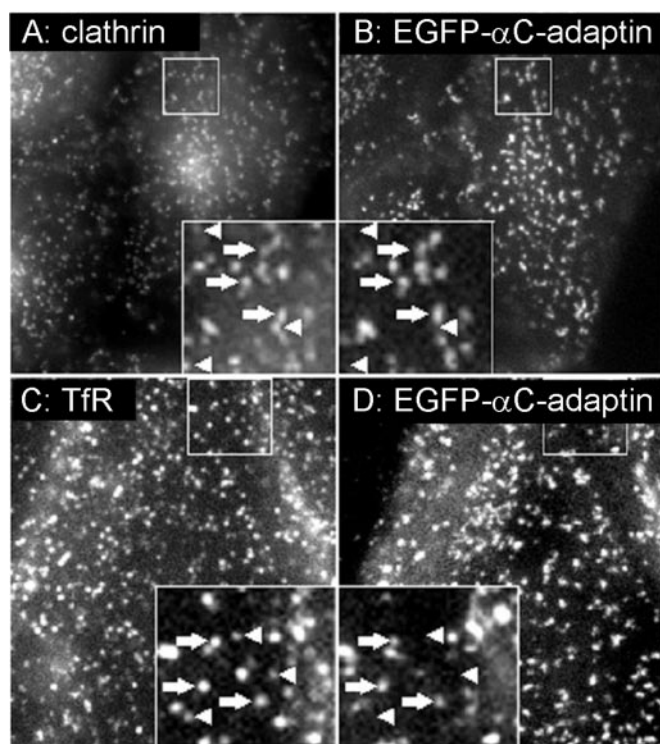


FIG. 1. Co-localization of EGFP- α C-adaptin in clathrin-coated pits. HeLa cells expressing EGFP- α C-adaptin (B and D) following immunocytochemistry performed using an antibody against clathrin light chain (A) or TfR (C) are shown. Three co-localized puncta are marked by *arrows*, and three puncta that do not contain EGFP- α C-adaptin are marked by *arrowheads*.

(Micomax, Princeton Instruments). Images were acquired with MetaMorph (Universal Imaging, Downingtown, PA) and processed with MetaMorph, NIH image (rsb.info.nih.gov/nih-image/) and Photoshop (Adobe Systems Inc., San Jose, CA).

Tf and LDL Uptake—Cells were placed in serum free DMEM for 30 min in a 37 °C incubator to chase out cell surface bound Tf or LDL. Cells were incubated for 30 min in AlexaFluor546-Tf or DiI-LDL (Molecular Probes) diluted 1:100 in serum free DMEM, rinsed two times in phosphate-buffered saline, and placed in DMEM with 10% fetal bovine serum for 30 min at 37 °C. Finally, cells were rinsed two times in phosphate-buffered saline and fixed for 5 min in 4% paraformaldehyde (Electron Microscopy Sciences, Fort Washington, PA). Epifluorescence imaging was performed as described previously (21, 25, 28). EGFP fluorescence was collected with a 515/30 band pass filter (500 ms exposure) and AlexaFluor546 or DiI emission with a 570lp long pass filter (100-ms exposure). All filters and dichroic mirrors were obtained from Chroma Technologies Corp. (Brattleboro, VT). Average fluorescence per pixel for each channel was calculated for each cell using MetaMorph.

TIR-FM Image Acquisition—TIR-FM was performed at 37 °C as described previously (21, 25, 28, 29). dsRed and EGFP simultaneous acquisition was performed utilizing an emission splitter (Dual-View, Optical Insights, LLC, Santa Fe, NM) equipped with a dichroic mirror to split the emission (550DCLP). The EGFP emission was then collected through an emission band pass filter (515/30) and the dsRed through an emission long pass filter (580lp).

Dual-color Processing—Dual-color TIR-FM image streams were aligned and correlation coefficients were calculated using MetaMorph, as described previously (25). The correlation coefficient is a pixel-by-pixel comparison of the intensity values between the two channels being analyzed and provides a relative numerical representation of co-localization. Correlation coefficients were obtained following pixel shift of the red image planes 1 pixel at a time for 10 pixels in each direction. Each of the four values for each pixel shift was averaged. Alignment was verified by an exponential decrease in correlation coefficient following pixel shift.

Calculation of Co-localization—200 dsRed-clathrin puncta were circled and average fluorescence was measured (50 per image). These regions were then transferred onto the corresponding EGFP- α C-adap-

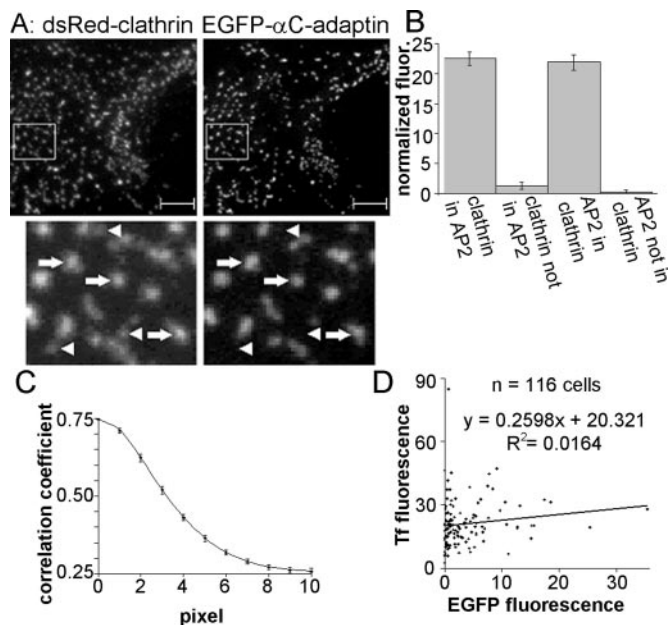


FIG. 2. Co-localization of EGFP- α C-adaptin and dsRed-clathrin at the plasma membrane. A, dual-color TIR-FM. Three co-localized puncta are marked by *arrows*, and three dsRed-clathrin puncta that do not contain EGFP- α C-adaptin are marked by *arrowheads*. Scale bars: 5 μ m. B, normalized dsRed-clathrin fluorescence from areas within EGFP- α C-adaptin spots and areas outside of EGFP- α C-adaptin spots and normalized EGFP- α C-adaptin fluorescence from areas within dsRed-clathrin spots and areas outside of dsRed-clathrin spots, $n = 200$ spots per group from at least 4 cells. C, pixel shift analysis comparing red and green channels. D, AlexaFluor546-Tf uptake in HeLa cell transfected with EGFP- α C-adaptin imaged via epi-fluorescence ($n = 116$ cells).

tin image, and average fluorescence was measured. The same was done for EGFP- α C-adaptin spots and for the corresponding locations on the dsRed-clathrin images. Additionally, this procedure was performed for regions that did not contain dsRed-clathrin spots and regions without EGFP- α C-adaptin spots. Normalized fluorescence for all dsRed-clathrin regions was calculated by subtracting from the average fluorescence of that region the mean average fluorescence of the 50 regions identified from that image as not containing a dsRed-clathrin spot. The same was done for each EGFP- α C-adaptin data point.

Calculation of Fluorescence in Static, Disappearing, and Mobile Spots—15 spots within each category were identified (5 per stream). The total fluorescence and area of the region of interest was obtained for each channel, as were the total fluorescence and area of a larger region surrounding the spot. The total fluorescence and area of the spot were then subtracted from the values for the larger region, and then the resultant fluorescence was divided by the area to obtain a value for average background fluorescence within an annulus surrounding each. Finally, each spot was normalized by dividing the average spot fluorescence per pixel by the average annulus fluorescence per pixel and then subtracting 1 from this number. For EGFP- α C-adaptin and dsRed-clathrin, the average spot area was 28.6 ± 1.1 pixels, and the average annulus area was 122.9 ± 14.5 pixels. For EGFP- β 2-adaptin and dsRed-clathrin, the average spot area was 23.9 ± 0.92 pixels, and the average annulus area was 80.1 ± 6.5 pixels.

RESULTS AND DISCUSSION

Previous studies have documented different populations of cell surface clathrin: static spots, mobile spots, and those that appeared to undergo endocytosis (17, 24, 25, 28). In our previous studies (25, 28) the clathrin puncta at the cell surface that disappeared into the cell ($\sim 15\%$ per min) or moved laterally in linear trajectories parallel to the plane of the plasma membrane ($\sim 2\%$ per min) represented a minority of the total. Thus, two general classes of plasma membrane associated clathrin can be defined, the dynamic and the static.

The AP-2 complex is a key player in the production of clathrin coats, forming the junction between internalized receptors

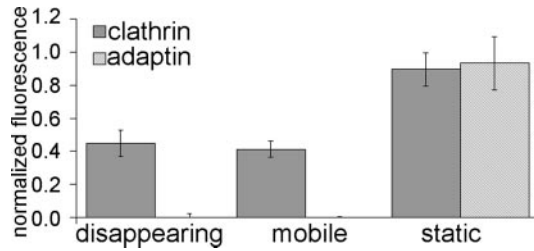


FIG. 3. dsRed-clathrin and EGFP- α C-adaptin fluorescence in disappearing, mobile, and static spots, $n = 15$ spots per group from at least three cells. Fluorescence is normalized to the local background fluorescence surrounding each spot at the image plane analyzed.

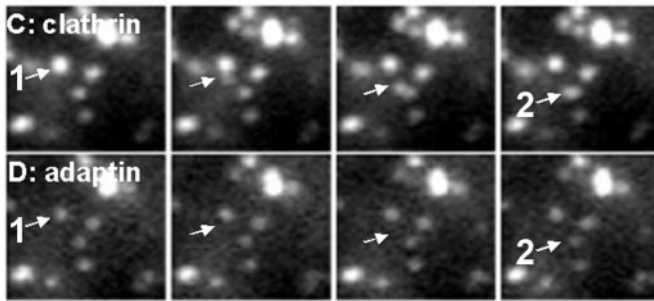
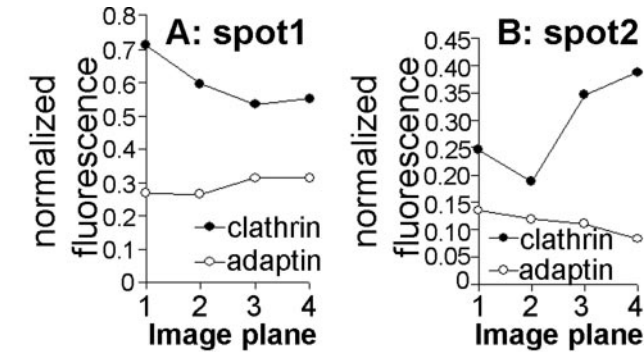


FIG. 4. Absence of α C-adaptin in dynamic clathrin spots. A and B, dsRed-clathrin and EGFP- α C-adaptin fluorescence, normalized to local background, at spots 1 and 2 from four image planes (presented in C and D). C and D, sequential image planes of dsRed-clathrin (C) and EGFP- α C-adaptin (D) (180-ms exposure time). The arrows in C and D track the motion of a dsRed-clathrin spot from spot 1 (arrow in first frame) to spot 2 (arrow in last frame).

and clathrin triskelia. To examine when and where the AP-2 complex engages the endocytic machinery, we expressed a subunit of the AP-2 complex, α -adaptin, as a fusion protein to EGFP. A similar fusion protein has recently been used as a marker for the AP-2 complex in FRAP (fluorescence recovery after photo-bleaching) studies (30) and appeared to exhibit wild-type function.

Following immunocytochemistry, many EGFP- α C-adaptin puncta co-localized with endogenous clathrin (Fig. 1, A and B), as well as other markers of clathrin-coated pits (clathrin, 96.7% co-localization; β -adaptin, 99.7%; Eps15, 98.9%; epsin, 97.7%; and CALM, 99.2%; in all cases $n > 375$ spots). Additionally, EGFP- α C-adaptin also co-localized with endogenous TfR suggesting its presence in active endocytic structures (Fig. 1, C and D; 94.1% co-localization, $n = 409$ spots). In contrast, γ -adaptin (a component of AP-1 and not AP-2) did not co-localize with EGFP- α C-adaptin (data not shown). When cells were co-transfected with dsRed-clathrin and EGFP- α C-adaptin and imaged simultaneously by TIR-FM, these two proteins appeared to co-localize in a large proportion of plasma membrane associated puncta (Fig. 2A). dsRed-clathrin intensity was significantly greater in puncta labeled with EGFP- α C-adaptin than

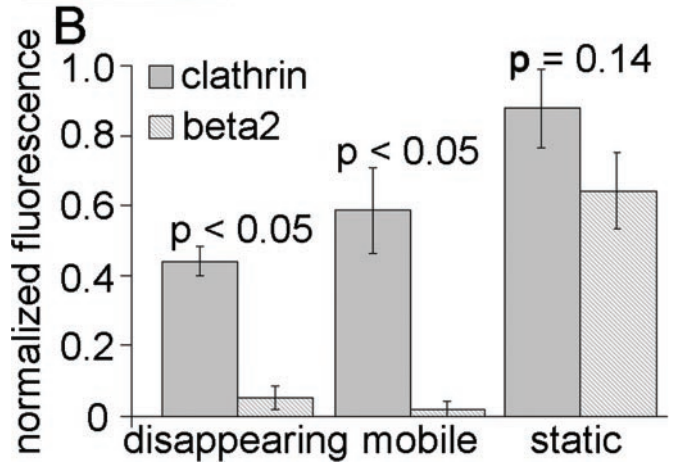
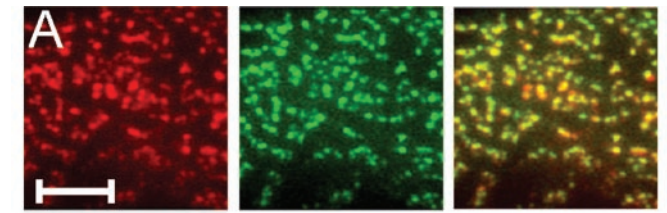


FIG. 5. Absence of β 2-adaptin in dynamic clathrin spots. A, overlay of dsRed-clathrin (red) and EGFP- β 2-adaptin (green) TIR-FM images. Scale bar: 5 μ m. B, normalized dsRed-clathrin and EGFP- β 2-adaptin fluorescence in disappearing, mobile and static spots, $n = 15$ spots per group from at least three cells. Fluorescence is normalized to the local background fluorescence surrounding each spot at the image plane analyzed.

in regions without EGFP- α C-adaptin puncta, and EGFP- α C-adaptin fluorescence was higher in regions containing dsRed-clathrin puncta than regions that did not (Fig. 2B). Additionally, quantification of the spatial correlation and the observation that the correlation coefficient decreased exponentially with deliberate misalignment of one image relative to the other indicated significant overlap between the α -adaptin and clathrin signals (Fig. 2C). Thus, EGFP- α C-adaptin co-localized in most, but not all, plasma membrane associated clathrin puncta.

To verify that EGFP- α C-adaptin does not affect clathrin-mediated endocytosis, we quantified the uptake of Alexa-Fluor546-Tf and DiI-conjugated low density lipoprotein (DiI-LDL) in cells transiently expressing this fusion protein. In these studies endocytosis did not seem to be significantly affected by the expression of EGFP- α C-adaptin (Fig. 2D and data not shown). Since EGFP- α C-adaptin localizes to clathrin-coated pits, and its expression does not adversely affect endocytosis, this fusion protein was used to study the spatial-temporal regulation of the AP-2 complex.

In contrast to the presence of a dynamic population of clathrin puncta (as quantified above), when EGFP- α C-adaptin was used to image AP-2, all puncta were static. This was observed consistently whether the EGFP- α C-adaptin was observed in single color mode or, when co-expressed with dsRed-clathrin, in simultaneous dual-color TIR-FM video imaging (Video 1 in the Supplemental Material).

These results led us to more specifically evaluate the co-localization between dsRed-clathrin and EGFP- α C-adaptin. When a total of 200 spots were analyzed from at least four co-transfected cells (50 per field), 99.5% of EGFP- α C-adaptin puncta were labeled with dsRed-clathrin. In contrast, only 89.5% of dsRed-clathrin puncta were labeled with EGFP- α C-adaptin (179/200: 25 out of 29 in the enlarged field in Fig. 2A). Similarly, in immunocytochemistry studies several puncta of

endogenous clathrin or TfR did not contain EGFP- α C-adaptin (arrowheads in Fig. 1). Thus, we hypothesized that clathrin devoid of AP-2 might represent the dynamic clathrin, puncta moving parallel to the coverslip or into the cell. To test this hypothesis we examined whether there were criteria that could distinguish dsRed-clathrin puncta that did or did not label with EGFP- α C-adaptin.

To evaluate the dsRed-clathrin that did not co-localize with EGFP- α C-adaptin, clathrin puncta were classified as static, mobile, or disappearing. Fifteen spots were identified from each category, and the dsRed-clathrin fluorescence was analyzed for each. Subsequently, the EGFP- α C-adaptin fluorescence at the same points in space and time was evaluated. Although, EGFP- α C-adaptin fluorescence was equal to dsRed-clathrin fluorescence in static spots, at the sites of disappearing or mobile spots the EGFP- α C-adaptin fluorescence was indistinguishable from the background fluorescence in annuli surrounding the puncta (Fig. 3). Thus, this analysis strongly suggests that the dsRed-clathrin puncta devoid of EGFP- α C-adaptin are the dynamic population.

In many cases moving dsRed-clathrin spots, without AP-2, appeared to originate from static puncta of clathrin and AP-2 (Fig. 4). A decrease in clathrin intensity was recorded (Fig. 4A) as part of a dsRed-clathrin spot moved away toward the second static spot (Fig. 4C). In contrast, the fluorescence of EGFP- α C-adaptin at the static spot did not decrease (Fig. 4, A and D). Additionally, although dsRed-clathrin fluorescence at the second spot increased as the mobile spot approached (Fig. 4B), the EGFP- α C-adaptin intensity at this location did not change.

The observation of mobile clathrin puncta emerging from static spots does not necessitate that they originated as a single unified structure. However, as the depth of penetration of the evanescent field is roughly equal to the diameter of a clathrin-coated pit (~ 100 nm), it is unlikely that these occurrences are the results of two distinct clathrin structures co-localizing in X and Y space relative to the plasma membrane but at different depths within the cell. The stepwise increase and decrease in clathrin spot fluorescence at the static points where dsRed-clathrin and EGFP- α C-adaptin co-localize before and after the observed motility (Fig. 4) suggests direct interactions between the static and mobile populations of clathrin. If they did indeed originate from separate puncta, it would still hold that the dynamic moving puncta are devoid of EGFP- α C-adaptin.

Our analysis (Figs. 1 and 2), as well as those of others (30), suggest that EGFP-tagged α -adaptin is a suitable marker for the AP-2 complex. However, we sought to test our observations with an alternate marker for AP-2 (β -adaptin), which when linked to green fluorescent protein (or yellow fluorescent protein) has also been reported to retain wild type function (31–33). In preliminary studies EGFP- β 2-adaptin did not seem to significantly decrease uptake of either AlexaFluor546-Tf or DiI-LDL (data not shown). In the LDL internalization assay some transfected cells did tend to have reduced endocytosis, although this finding was not statistically significant ($R^2 = 0.0358$).

TIR-FM performed on cells co-expressing dsRed-clathrin and EGFP- β 2-adaptin demonstrated significant co-localization (Fig. 5A), and video microscopy confirmed the relative static nature of β 2-adaptin-labeled AP-2 compared with clathrin. Although a few dynamic clathrin spots appeared to contain some EGFP- β 2-adaptin, as with EGFP- α C-adaptin, the vast majority of both disappearing and mobile spots were devoid of detectable AP-2 (Fig. 5B). Quantification demonstrated that the EGFP- β 2-adaptin present at the site of 15 disappearing or

mobile clathrin spots was not significantly different from local background. In contrast, static spots contained nearly equivalent amounts of clathrin and AP-2 (Fig. 5B). Thus, these results verify our previous observations with EGFP- α C-adaptin.

While co-localization was observed between clathrin and AP-2 for a majority of spots, a static analysis does not represent the entire story. Our observations show that the minority of clathrin spots devoid of AP-2 are the clathrin puncta moving either parallel, or perpendicular, to the plasma membrane. This suggests that static co-localized puncta of clathrin and AP-2 may serve as loci for the formation of clathrin-coated pits. It is possible that the dynamic population of clathrin represents clathrin-coated vesicles that contain AP-2, but that the AP-2 is polarized toward the cytosolic side of the nascent vesicle, out of the evanescent field. However, as the depth of penetration of the evanescent field employed in these studies approximates the diameter of a clathrin-coated vesicle (~ 100 nm), this is probably not the case.

The observation that AP-2 does not remain with clathrin puncta that start to move was not predicted in light of current models which suggest that the AP-2 complex remains within clathrin-coated vesicles subsequent to fission from the plasma membrane (10, 11, 16). However, as these studies represent the first live cell imaging of the AP-2 complex during endocytosis, we currently have no information with which to directly compare our observations.

REFERENCES

- Bretscher, M. S. (1996) *Cell* **87**, 601–606
- Conrad, M. E., Umbreit, J. N., and Moore, E. G. (1999) *Am. J. Med. Sci.* **318**, 213–229
- Hopkins, C. R., Miller, K., and Beardmore, J. M. (1985) *J. Cell Sci. Suppl.* **3**, 173–186
- Lamaze, C., and Schmid, S. L. (1995) *J. Cell Biol.* **129**, 47–54
- Raub, T. J., and Kuentzel, S. L. (1989) *Exp. Cell Res.* **184**, 407–426
- Slepnev, V. I., and De Camilli, P. (2000) *Nat. Rev. Neurosci.* **1**, 161–172
- Sorkin, A., and von Zastrow, M. (2002) *Nat. Rev. Mol. Cell Biol.* **3**, 600–614
- Brodsky, F. M., Chen, C. Y., Knuehl, C., Towler, M. C., and Wakeham, D. E. (2001) *Annu. Rev. Cell Dev. Biol.* **17**, 517–568
- Conner, S. D., and Schmid, S. L. (2003) *Nature* **422**, 37–44
- Schmid, S. L. (1997) *Annu. Rev. Biochem.* **66**, 511–548
- Takei, K., and Haucke, V. (2001) *Trends Cell Biol.* **11**, 385–391
- Kirchhausen, T. (1999) *Annu. Rev. Cell Dev. Biol.* **15**, 705–732
- Pearse, B. M. (1976) *Proc. Natl. Acad. Sci. U. S. A.* **73**, 1255–1259
- Steer, C. J., Klausner, R. D., and Blumenthal, R. (1982) *J. Biol. Chem.* **257**, 8533–8540
- Takei, K., Haucke, V., Slepnev, V., Farsad, K., Salazar, M., Chen, H., and De Camilli, P. (1998) *Cell* **94**, 131–141
- Kirchhausen, T. (2002) *Cell* **109**, 413–416
- Gaidarov, I., Santini, F., Warren, R. A., and Keen, J. H. (1999) *Nat. Cell Biol.* **1**, 1–7
- Santini, F., Gaidarov, I., and Keen, J. H. (2002) *J. Cell Biol.* **156**, 665–676
- Scott, M. G., Benmerah, A., Muntaner, O., and Marullo, S. (2002) *J. Biol. Chem.* **277**, 3552–3559
- Axelrod, D. (1981) *J. Cell Biol.* **89**, 141–145
- Schmoranzler, J., Goulian, M., Axelrod, D., and Simon, S. M. (2000) *J. Cell Biol.* **149**, 23–32
- Toomre, D., and Manstein, D. J. (2001) *Trends Cell Biol.* **11**, 298–303
- Licht, S. S., Sonnleitner, A., Weiss, S., and Schultz, P. G. (2003) *Biochemistry* **42**, 2916–2925
- Merrifield, C. J., Feldman, M. E., Wan, L., and Almers, W. (2002) *Nat. Cell Biol.* **4**, 691–698
- Rappoport, J. Z., and Simon, S. M. (2003) *J. Cell Sci.* **116**, 847–855
- Benmerah, A., Bayrou, M., Cerf-Bensussan, N., and Dautry-Varsat, A. (1999) *J. Cell Sci.* **112**, 1303–1311
- Benmerah, A., Poupon, V., Cerf-Bensussan, N., and Dautry-Varsat, A. (2000) *J. Biol. Chem.* **275**, 3288–3295
- Rappoport, J. Z., Taha, B. W., and Simon, S. M. (2003) *Traffic* **4**, 460–467
- Lampson, M. A., Schmoranzler, J., Zeigerer, A., Simon, S. M., and McGraw, T. E. (2001) *Mol. Biol. Cell* **12**, 3489–3501
- Wu, X., Zhao, X., Puertollano, R., Bonifacino, J. S., Eisenberg, E., and Greene, L. E. (2003) *Mol. Biol. Cell* **14**, 516–528
- Jiang, X., Huang, F., Marusyk, A., and Sorkin, A. (2003) *Mol. Biol. Cell* **14**, 858–870
- Laporte, S. A., Oakley, R. H., Zhang, J., Holt, J. A., Ferguson, S. S., Caron, M. G., and Barak, L. S. (1999) *Proc. Natl. Acad. Sci. U. S. A.* **96**, 3712–3717
- Sorkina, T., Huang, F., Beguinot, L., and Sorkin, A. (2002) *J. Biol. Chem.* **277**, 27433–27441